

## Supplementary Information

### Liver-specific deletion of ROR $\alpha$ aggravates diet-induced nonalcoholic steatohepatitis by inducing mitochondrial dysfunction

Hyeon-Ji Kim<sup>1</sup>, Yong-Hyun Han<sup>1</sup>, Hyelin Na<sup>1</sup>, Ju-Yeon Kim<sup>1</sup>, Taewook Kim<sup>2</sup>, Hye-Jin Kim<sup>1</sup>,  
Chanseok Shin<sup>2</sup>, Jung Weon Lee<sup>1,4</sup>, and Mi-Ock Lee<sup>1,3,4</sup>

<sup>1</sup>College of Pharmacy, Seoul National University, Seoul, Korea; <sup>2</sup>Department of Agricultural Biotechnology, Seoul National University, Seoul, Republic of Korea; <sup>3</sup>Bio-MAX institute, Seoul National University, Seoul, Korea; <sup>4</sup>Research Institute of Pharmaceutical Sciences, Seoul, Republic of Korea

## Supplementary Methods

### RNA-seq and ChIP-seq analyses

The RNA used in sequencing analysis was obtained from the liver tissues of HFD-fed ROR $\alpha$ -LKO and ROR $\alpha$ <sup>f/f</sup> mice. For control and test RNAs, the construction of a library was performed using a SENSE mRNA-Seq Library Prep Kit (Lexogen, Inc., Austria), according to the manufacturer's instructions. High-throughput sequencing was performed as paired-end 100 sequencing using HiSeq 2500 (Illumina, Inc., USA). RNA-Seq reads were mapped using the TopHat software tool, to obtain the alignment file. The alignment file was used for assembling transcripts, estimating their abundance, and detecting the differential expression

of genes or isoforms using cufflinks. Gene classification was based on searches of the BioCarta (<http://www.biocarta.com/>), GenMAPP (<http://www.genmapp.org/>), DAVID (<http://david.abcc.ncifcrf.gov/>), and Medline databases (<http://www.ncbi.nlm.nih.gov/>). The GO analysis was performed in DAVID Bioinformatics Resources 6.7. ROR $\alpha$  ChIP-seq (GSE59486) and liver input control (GSE26345) were downloaded from gene expression omnibus (GEO) (<http://www.ncbi.nlm.nih.gov/geo>)<sup>1,2</sup>. A public ChIP-seq is conducted in C57BL/6 mouse liver. Low-quality small RNA reads and adapter sequences were removed using FASTX-Toolkit ([http://hannonlab.cshl.edu/fastx\\_toolkit/](http://hannonlab.cshl.edu/fastx_toolkit/)). Analysis was performed as previously described<sup>2</sup>. High-quality reads were aligned with the mouse reference genome (mm9) using Bowtie v1.1.2 with options ‘-n 2 -l 34 --best --strata -m 1’<sup>3</sup>. Only uniquely aligned reads to the genome were chosen for further analysis. Peak calling was performed using HOMER and a published liver input control<sup>4</sup>. Peaks were filtered according to two criteria: (1) score  $\geq 10$  and (2) peaks between -100 kb from transcription start site (TSS) and TSE. ChIP-seq peaks were visualized in IGV<sup>5</sup>.

### **Analysis of mitochondrial mass using flow cytometry**

Primary hepatocytes were isolated and incubated with low glucose DMEM media containing 100 nM MitoTracker green FM (Invitrogen) for 30 min. Green fluorescence was detected by flow cytometry.

### **Accession number**

Raw data for HFD-fed control and ROR $\alpha$ -LKO mouse RNA-seq are available in GSE90844.

**Supplementary Table.**

Gene	Accession number		Nucleotide sequence	Species	Purpose
ROR $\alpha$	NM_013646.2	Sense	5'-TTTCAGGAGAAGTCAGCAGAG-3'	Mouse	qRT-PCR primer
	NM_001289916.1	Antisense	5'-TCTGCTGGTCCGATCAATCAA-3'		
ROR $\beta$	NM_001043354.2	Sense	5'-ATGGCAGACCCACACCTACG-3'	Mouse	
	NM_146095.4	Antisense	5'-TATCCGCTTGGCGAACTCC-3'		
ROR $\gamma$	NM_011281.3	Sense	5'-CGAGATGCTGTCAAGTTTGGC-3'	Mouse	
	NM_001293734.1	Antisense	5'-TGTAAGTGTGTCTGCTCCGCG-3'		
LXR $\alpha$	NM_001177730.1	Sense	5'-AGGAGTGTGCGACTTCGCAA-3'	Mouse	
	NM_013839.4	Antisense	5'-CTCTTCTTGCCGCTTCAGTTT-3'		
Fasn	NM_007988.3	Sense	5'-CATGACCTCGTGATGAACGTGT-3'	Mouse	
		Antisense	5'-CGGGTGAGGACGTTTACAAAG-3'		
SCD1	NM_009127.4	Sense	5'-AGATCTCCAGTTCTTACACGACCAC-3'	Mouse	
		Antisense	5'-GACGGATGTCTTCTCCAGGTG-3'		
Acly	NM_001199296.1	Sense	5'-GATGAAAGTGGCACCTGCAAAG-3'	Mouse	
	NM_134037.3	Antisense	5'-GGTATGTCGGCTGAAGAGGGT-3'		
Acaca	NM_133360.2	Sense	5'-GCGGGAGGAGTTCCTAATTC-3'	Mouse	
		Antisense	5'-GGTTGGCATTGTGGATTTTC-3'		
CD36	NM_001159558.1	Sense	5'-TCCTCTGACATTTGCAGGTCTATC-3'	Mouse	
	NM_001159557.1	Antisense	5'-AAAGGCATTGGCTGGAAGAA-3'		
TNF $\alpha$	NM_013693.3	Sense	5'-AATGGCCTCCCTCTCATCAGTT-3'	Mouse	
		Antisense	5'-CCACTTGGTGGTTTGCTACGA-3'		
NLRP3	NM_145827.3	Sense	5'-AGCCTTCCAGGATCCTCTTC-3'	Mouse	
		Antisense	5'-CTTGGGCAGCAGTTCTTTTC-3'		
IL-1 $\beta$	NM_008361.4	Sense	5'-AGAGCCCATCCTCTGTGACTCA-3'	Mouse	
		Antisense	5'-TGCTTGGGATCCACACTCTCCA-3'		
Col1a1	NM_007742.4	Sense	5'-GACATCCCTGAAGTCAGCTGC-3'	Mouse	
		Antisense	5'-TCCCTTGGGTCCCTCGAC-3'		
$\alpha$ -SMA	NM_007392.3	Sense	5'-GGCACCACTGAACCCTAAGG-3'	Mouse	
		Antisense	5'-TCTCCAGAGTCCAGCACAAT-3'		
TGF $\beta$	NM_011577.2	Sense	5'-CGACATGGAGCTGGTGA-3'	Mouse	
		Antisense	5'-TCCCGAATGTCTGACGTA-3'		
MMP-2	NM_008610.3	Sense	5'-TTTGCTCGGGCCTTAAAAGTAT-3'	Mouse	
		Antisense	5'-CCATCAAATGGGTATCCATCTC-3'		
TIMP1	NM_001294280.2	Sense	5'-CTTGGTTCCCTGGCGTACTC-3'	Mouse	
	NM_011593.2	Antisense	5'-ACCTGATCCGTCCACAAACAG-3'		
Bnip3	NM_009760.4	Sense	5'-CTCCAGACACCACAAGATAC-3'	Mouse	
		Antisense	5'-CTTCTCAGACAGAGTGCTG-3'		
Drp1	NM_152816.3	Sense	5'-CGTGACAAATGAAATGGTGC-3'	Mouse	
	NM_001025947.2	Antisense	5'-CATTAGCCACAGGCATCAG-3'		
Fis1	NM_001276340.1			Mouse	
	NM_001276341.1				
Fis1	NM_025562.3	Sense	5'-AGGCTCTAAAGTATGTGCGAGG-3'	Mouse	
	NM_001163243.1	Antisense	5'-GGCCTTATCAATCAGGCGTTC-3'		
Pink1	NM_026880.2	Sense	5'-GCTTGCCAATCCCTTCTATG-3'	Mouse	
		Antisense	5'-CTCTCGCTGGAGCAGTGAC-3'		
Mfn1	NM_024200.4	Sense	5'-CCTACTGCTCCTTCTAACCCTA-3'	Mouse	
		Antisense	5'-AGGGACGCCAATCCTGTGA-3'		
Mfn2	NM_001285920.1	Sense	5'-AGAAGTGGACCCGGTTACCA-3'	Mouse	
	NM_133201.3	Antisense	5'-CACTTCGCTGATACCCCTGA-3'		
Mfn2	NM_001285921.1			Mouse	
	NM_001285922.1				
Mfn2	NM_001285923.1			Mouse	

OPA1	NM_001199177.1	Sense Antisense	5'-CTGAGGCCCTTCTCTTGTTAGG-3' 5'-CTGACACCTTCCTGTAATGCTTG-3'	Mouse	
PGC-1 $\alpha$	NM_008904.2	Sense Antisense	5'-CCCTGCCATTGTTAAGACC-3' 5'-TGCTGCTGTTCTGTTTTTC-3'	Mouse	
TFAM	NM_009360.4	Sense Antisense	5'-GGAATGTGGAGCGTGCTAAAA-3' 5'-ACAAGACTGATAGACGAGGGG-3'	Mouse	
Idha	NM_029573.2	Sense Antisense	5'-CCTCCTGCTTAGTGCTGTGA-3' 5'-CGTTGCCTCCCAGATCTTT-3'	Mouse	
Acadm	NM_007382.5	Sense Antisense	5'-GATCGCAATGGGTGCTTTTGATAGAA-3' 5'-AGCTGATTGGCAATGCTCCAGCAAA-3'	Mouse	
ND1	NC_005089.1 NC_006914.1	Sense Antisense	5'-ACGCAAAATCTTAGGGTACA-3' 5'-GAGTGATAGGGTAGGTGCAA-3'	Mouse	
COX1	NC_005089.1 NC_006914.1	Sense Antisense	5'-ATTTCGAGCAGAATTAGGTCA-3' 5'-CTCCGATTATTAGTGGGACA-3'	Mouse	
Ndufv1	NM_025523.1	Sense Antisense	5'-TTCCTCTGGATTACCCCTCA-3' 5'-CATGAGGAGCGCGAGTATTT-3'	Mouse	
Sdha	NM_023281.1	Sense Antisense	5'-GAAAGGCGGGCAGGCTCATC-3' 5'-CACCACGGCACTCCCATTTC-3'	Mouse	
Uqcr	NM_025650.2	Sense Antisense	5'-TGCCGAGGCCTCAGACACAG-3' 5'-TCCAAGGCATAAGAATAAGGTTT-3'	Mouse	
Cox5a	NM_007747.2	Sense Antisense	5'-TTGATGCCTGGGAATTGCGTAAAG-3' 5'-ACAACCTCCAAGATGCGAACAG-3'	Mouse	
Atp5g1	NM_007506.6 NM_001161419.1	Sense Antisense	5'-AGTTGGTGTGGCTGGATCA-3' 5'-GCTGCTTGAGAGATGGGTTC-3'	Mouse	
CytC	NM_007808.4	Sense Antisense	5'-GGAGGCAAGCATAAGACTGG-3' 5'-TCCATCAGGGTATCCTCTCC-3'	Mouse	
18s rRNA	NR_003278.3	Sense Antisense	5'-GTAACCCGTTGAACCCATT-3' 5'-CCATCCAATCGGTAGTAGCG-3'	Mouse	
Reads-enriched region in Bnip3		Sense Antisense	5'-GAAACTGGCGTGATGAAATCTT-3' 5'-GATCTCACTTTCAGCCAAC-3'	Mouse	
Reads-enriched region in PGC-1 $\alpha$		Sense Antisense	5'-CGGAGCTGCTAACTAACAATGG-3' 5'-GATGTGTATCACTGCACCACAC-3'	Mouse	ChIP primer
I		Sense Antisense	5'-GTGTGGTGAAGAGTGAGGAT-3' 5'-AGGATTGCTATGAGCCTCTG-3'	Mouse	
II		Sense Antisense	5'-GGCCCTGCCTGATCTTTAG-3' 5'-GAGCACACAAACAAGAAGTTAGG-3'	Mouse	
III		Sense Antisense	5'-TTGTGTATACCACCACAAGTGCACC-3' 5'-AGTACAGGACACTTCGGTGTCTACC-3'	Mouse	Genotyping primer
ROR $\alpha^{P1}$ allele (P1 and P2)		Sense Antisense	5'-TTGTGTATACCACCACAAGTGCACC-3' 5'-AGTACAGGACACTTCGGTGTCTACC-3'	Mouse	Genotyping primer
Alb <sup>Cre</sup> allele (Cre)		Sense Antisense	5'-TACAGACTGTGAGCAGATGTTTC-3' 5'-TTCTTGCGAACCTCATCACTCGTTG-3'	Mouse	Genotyping primer
RORE/Bnip3		Sense Antisense	5'-CCCAACTGGGACGCCCAACTGGGACGC CCAAGTGGGACGCG-3' 5'-CTAGCGCGTCCCAGTTGGGCGTCCCAG TTGG GCGTCCCAGTTGGGAGCT-3'		Cloning
RORE(I)/PGC-1 $\alpha$		Sense Antisense	5'-CGGGAGGGTCAAGTGGGAGGGTCAAGT GGGAGGGTCAAGTG-3' 5'-CTAGCACTTGACCCTCCCCTTGACCC TCCCCTTGACCCTCCCAGCT-3'		Cloning

Supplementary Figures

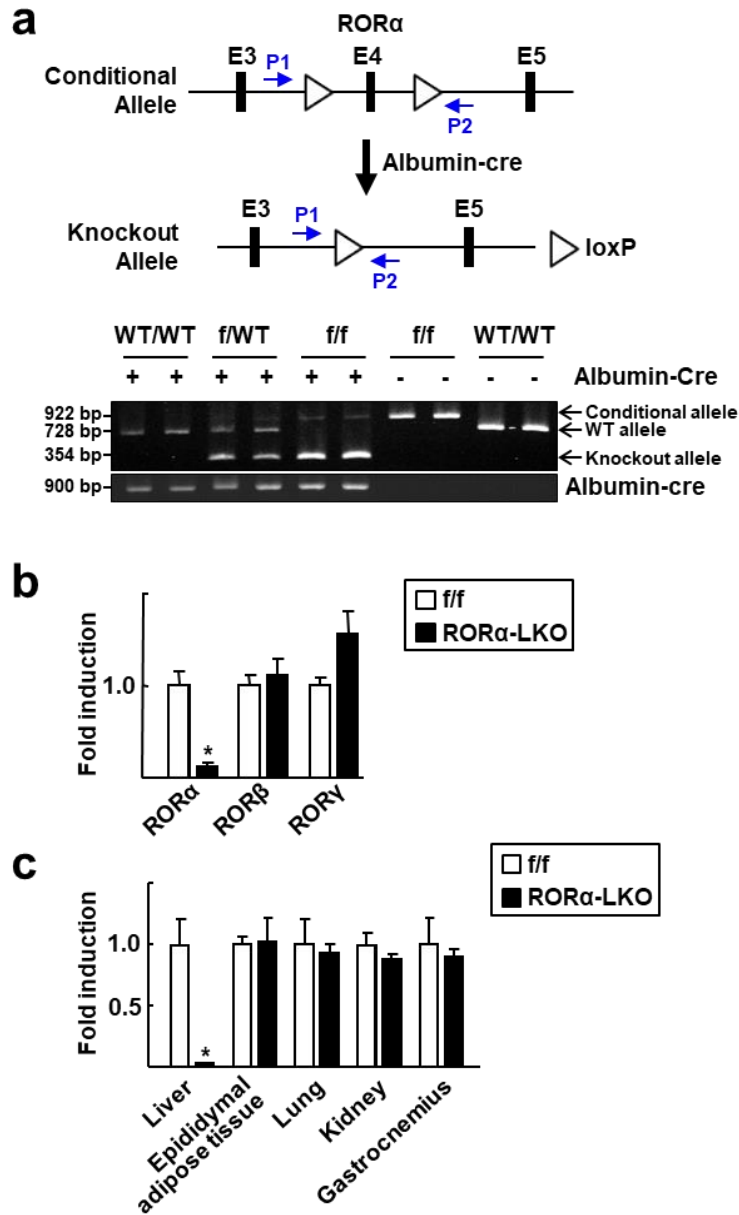


**Figure S1. Generation and characterization of the liver-specific RORα knockout mice.**

(a) Schematic representation of the conditional RORα floxed allele and the strategy of generation of the liver-specific RORα-deficient allele through Albumin-Cre recombination. E; Exon (upper). Genotyping analysis of the RORα<sup>f/f</sup> and Alb<sup>Cre</sup>-RORα<sup>f/f</sup> (RORα-LKO) mice. The primer sequences (P1/P2 and Cre) used for the genotyping were shown in Table (lower).

(b) The mRNA expression levels of the RORα, RORβ, and RORγ in liver tissues were measured by qRT-PCR. Values represent mean ± SEM. \*P < 0.05 vs RORα<sup>f/f</sup> (n=4).

(c) The relative mRNA expression levels of RORα in various tissues. Values represent mean ± SEM. \*P < 0.05 vs RORα<sup>f/f</sup> (n=4).

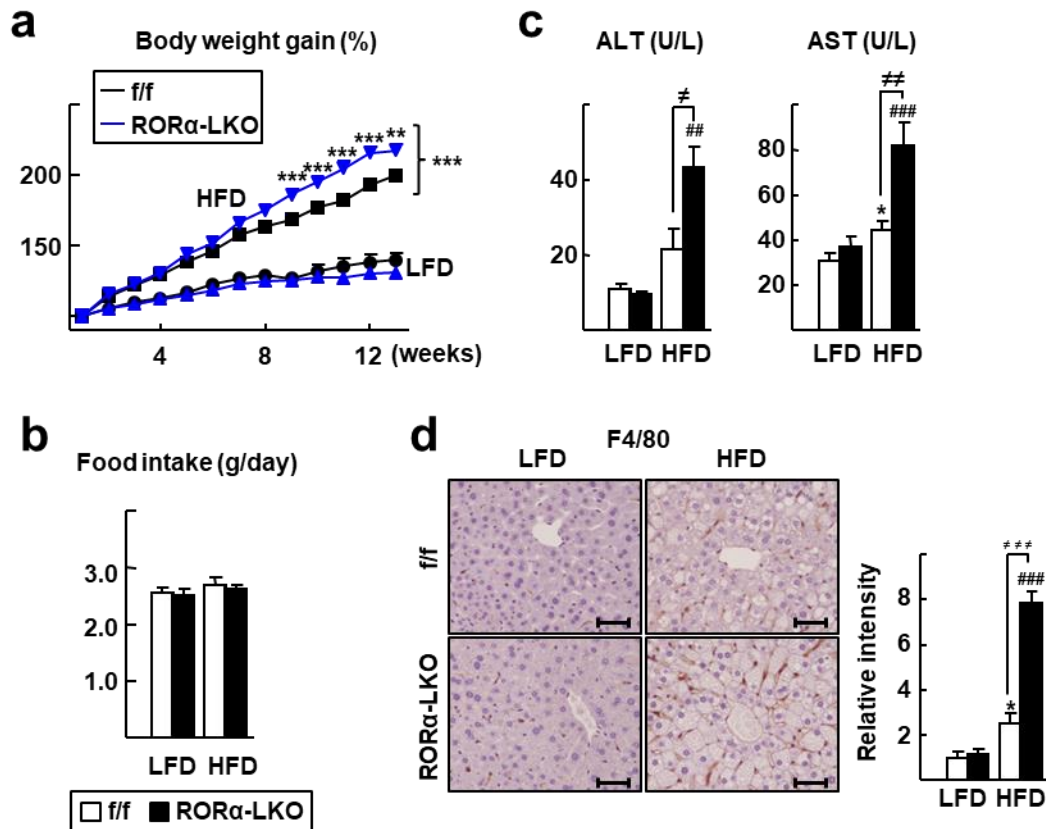


**Figure S2. Liver-specific KO of ROR $\alpha$  exacerbates the HFD-induced body weight gain and liver injury.**

(a) Six week-old ROR $\alpha$ -LKO and ROR $\alpha^{f/f}$  mice were fed with either LFD or HFD for 12 weeks. Body weight gain (%) represents the % increase compared to initial body weight (ranged from 17.0g to 23.6g). Data represent as mean  $\pm$  SEM. \*\* $P < 0.01$ , \*\*\* $P < 0.001$  vs HFD-fed ROR $\alpha^{f/f}$  (n=7-9).

(b) Food intake (g/day). Data represent as mean  $\pm$  SEM.

(c) Serum ALT and AST activities were measured by standard clinical chemistry assays at the end of experiments. Data presented as mean  $\pm$  SEM (n=7-9). ALT; ### $P < 0.01$  vs LFD-fed ROR $\alpha$ -LKO,  $^{\#}P < 0.05$  vs HFD-fed ROR $\alpha^{f/f}$ , AST; \* $P < 0.05$  vs LFD-fed ROR $\alpha^{f/f}$ , ### $P < 0.001$  vs LFD-fed ROR $\alpha$ -LKO,  $^{##}P < 0.01$  vs HFD-fed ROR $\alpha^{f/f}$ .

(d) Histological staining of F4/80. Scale bar: 50  $\mu$ m. Representative Images of liver sections from the ROR $\alpha^{f/f}$  and ROR $\alpha$ -LKO mice were presented. Relative intensities were quantified using ImageJ. Values represent mean  $\pm$  SEM (n=6-8). \* $P < 0.05$  vs LFD-fed ROR $\alpha^{f/f}$ , ### $P < 0.001$  vs LFD-fed ROR $\alpha$ -LKO,  $^{##}P < 0.001$  vs HFD-fed ROR $\alpha^{f/f}$ .

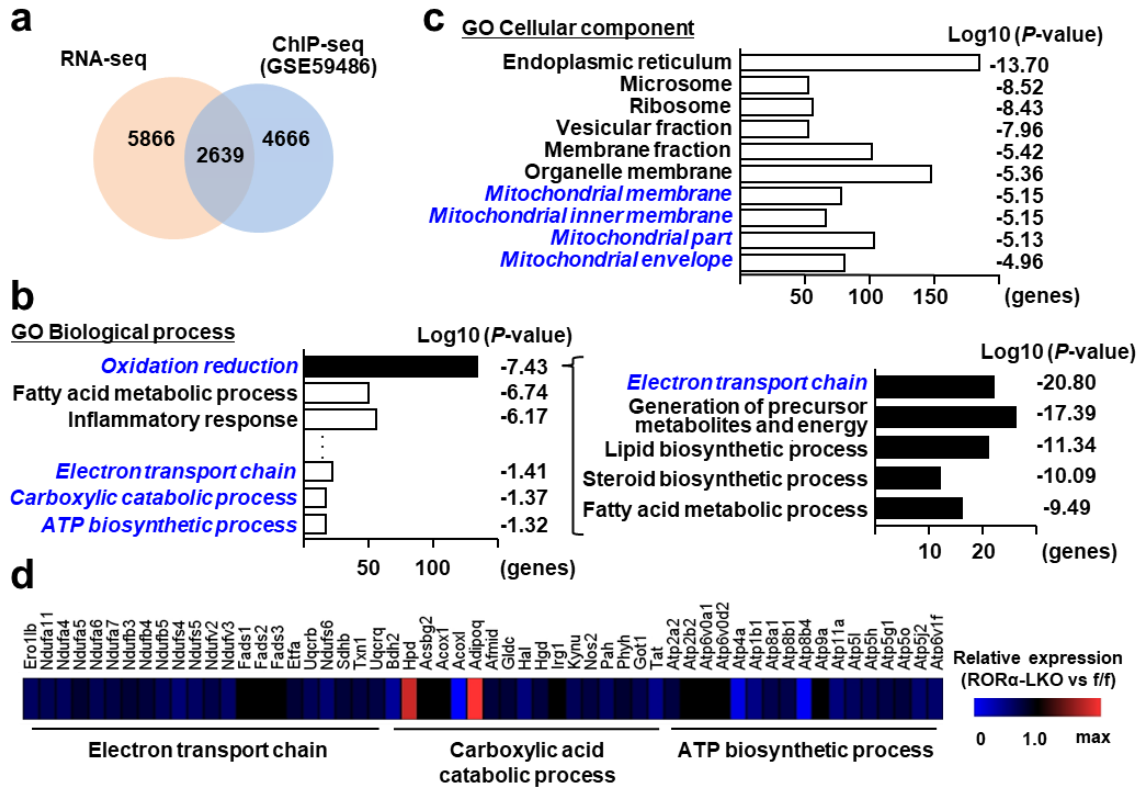


**Figure S3. Gene expression profiling for liver tissues from the ROR $\alpha$ -LKO mice.**

(a) Venn diagrams showing the overlapping target genes those delineated by the RNA-seq analysis in this study and the publically available ChIP-seq dataset (Fang *et al*, 2014). RNA-seq data was obtained from liver tissues of ROR $\alpha$ -LKO and ROR $\alpha^{f/f}$  mice and the fold change of each gene was calculated by dividing the normalized read count of HFD-fed ROR $\alpha$ -LKO by that of ROR $\alpha^{f/f}$ . (cut-off: 0.8-fold, 1.5-fold).

(b) GO biological process analysis for the overlapped genes (left). Genes clustered in the top ranked GO biological process term, oxidation reduction, were further analyzed for GO biological process analysis. Top 5 GO based on P-value are shown (right).

(c) GO cellular component analysis for the overlapped genes. Bar graph showing the top 10 enriched cellular component based on P-value. The number of genes in each ontology category is shown.

(d) Heat map representation of differentially regulated genes associated with electron transport, carboxylic acid catabolic process, and ATP biosynthetic process. Gene symbols are indicated.

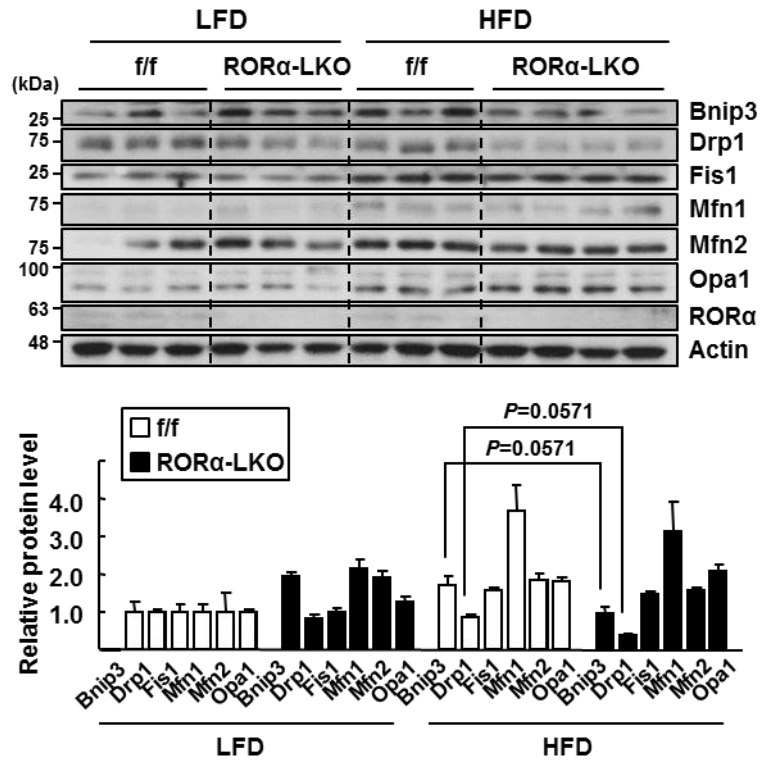


**Figure S4. The expression levels of Bnip3 and Drp1 were decreased in the HFD-fed RORα-LKO with marginal significances.**

The levels of indicated proteins were analyzed by western blotting (upper). Band intensities of each protein were quantified using ImageJ and normalized to that of actin (lower). Data presented as mean  $\pm$  SEM (n=3-4).

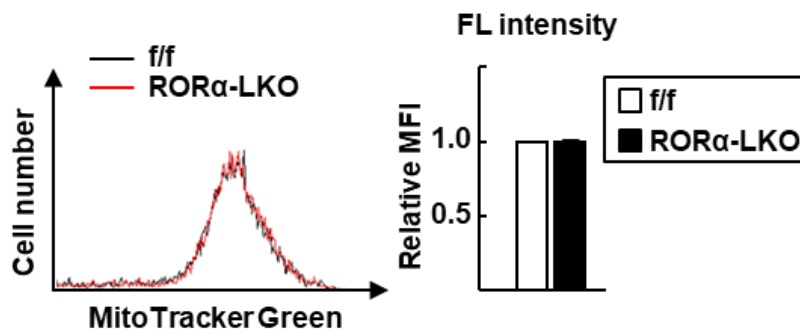


**Figure S5. Analysis of mitochondrial mass using flow cytometry.**

Primary hepatocytes were isolated from control and ROR $\alpha$ -LKO mice and were incubated with 100nM MitoTracker Green FM (Invitrogen) for 30 min. Green fluorescence was detected by flow cytometry (left) and relative mean fluorescence intensity (MFI) of stained cells was presented. Data presented as mean  $\pm$  SEM (n=3).

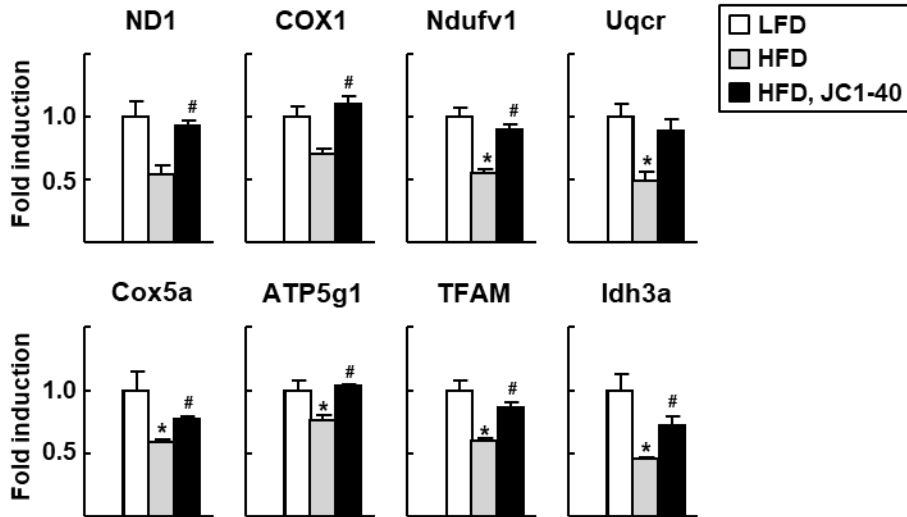


**Figure S6. Administration of JC1-40 restores the expression level of mitochondrial OXPHOS genes in the HFD-fed mice.**

Six weeks-old C57BL/6 mice were fed with either LFD or HFD for 12 weeks. After 7 weeks, JC1-40 was administered daily at doses of 5 mg/kg/day by oral gavage for 5 weeks. The expression levels of mitochondrial OXPHOS and genes related to mitochondrial biogenesis were analyzed by qRT-PCR. Data presented as mean  $\pm$  SEM (n=4). \* $P < 0.05$  vs LFD-fed mice and # $P < 0.05$  vs HFD-fed mice. ND1, NADH-ubiquinone oxidoreductase chain 1; COX1, Cytochrome c oxidase 1; Ndufv1, NADH dehydrogenase [ubiquinone] flavoprotein 1, mitochondrial; Uqcr, ubiquinol-cytochrome c reductase, complex 3 subunit 11; Cox5a, Cytochrome c oxidase subunit 5a; ATP5g1, ATP synthase lipid-binding protein, mitochondrial; TFAM, Mitochondrial transcription factor A; Idh3a, Isocitrate dehydrogenase [NAD] subunit alpha, mitochondrial.

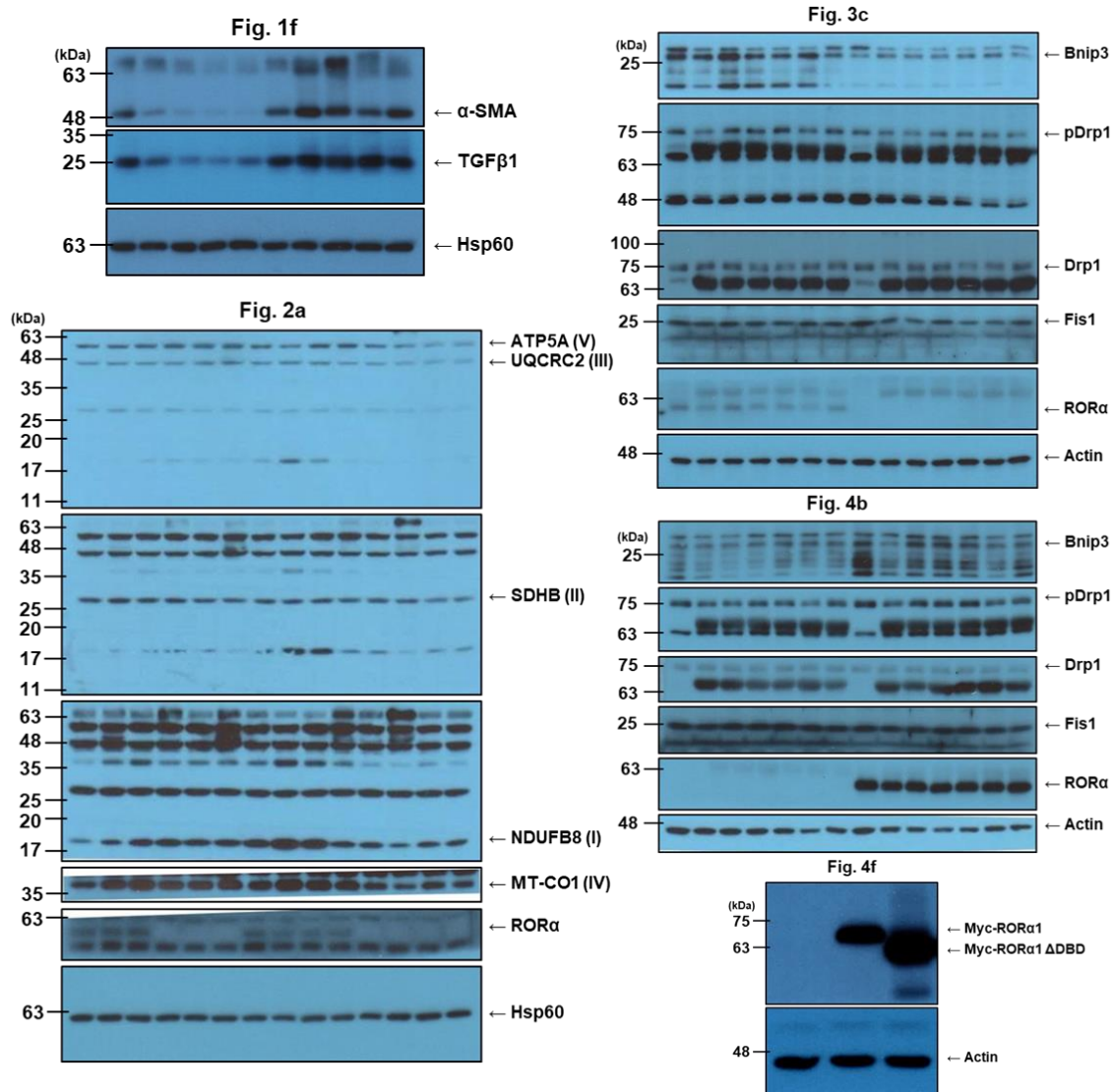


**Figure S7. The original images of blots presented in the main figures.**

The original images of the main figures are presented and the numbers in the left side of the blot indicate the molecular mass of each protein.

## References

1. Fang, B. *et al.* Circadian enhancers coordinate multiple phases of rhythmic gene transcription in vivo. *Cell* **159**, 1140-1152 (2014).
2. Feng, D. *et al.* A circadian rhythm orchestrated by histone deacetylase 3 controls hepatic lipid

- metabolism. *Science* **331**, 1315–1319 (2011).
3. Langmead, B., Trapnell, C., Pop, M. & Salzberg, S. L. Ultrafast and memory-efficient alignment of short DNA sequences to the human genome. *Genome Biol.* **10**, R25 (2009).
  4. Heinz, S. *et al.* Simple combinations of lineage determining transcription factors prime cis-regulatory elements required for macrophage and B cell identities. *Mol. Cell* **38**, 576–589 (2010).
  5. Robinson, J. T. *et al.* Integrative genomics viewer. *Nat. Biotechnol.* **29**, 24–26 (2011).